20.334 Biological Systems Modeling
Final Paper

Rishabh Datta
October 20th, 2019

Introduction

This project involves the modeling and design of a microfluidic biosensor system. Target nucleotides present in the bulk solution bind to complementary DNA sequences on a binding patch located on the bottom of the microchannel. The binding and complex formation is characterized by a second-order diffusion reaction as shown:

$$Ab + A \leftrightarrow AbA$$

Here, Ab represents the receptors or DNA sequences on the binding patch, and A represents the target molecules in the sample, and AbA is the bound complex formed. In this report, the effect of microchannel height d on the total number of bound complexes is investigated in both velocity-driven and pressure-driven flows. Next, the effect of association and dissociation rates on total binding at the patch is investigated; and finally, the effect of different microchannel designs with varying channel diameters is considered to maximize the total binding at the biosensor patch.

Methodology

Geometry and Meshing. A 2D model of the biosensor system as shown in Figure 1is used for the current modeling. The geometry is discretized using a variable-density mesh comprised of 2D triangular elements, as shown in Figure 1. The mesh density is higher at corners and near the surfaces, which represent geometric discontinuities. Since geometric discontinuities can prevent convergence of the solution, a higher mesh density is used in these regions. A higher mesh density is also used at the walls to appropriately resolve the boundary layers required for the laminar flow model. The problem is also a multi-scale problem, since the height of the microchannel is much

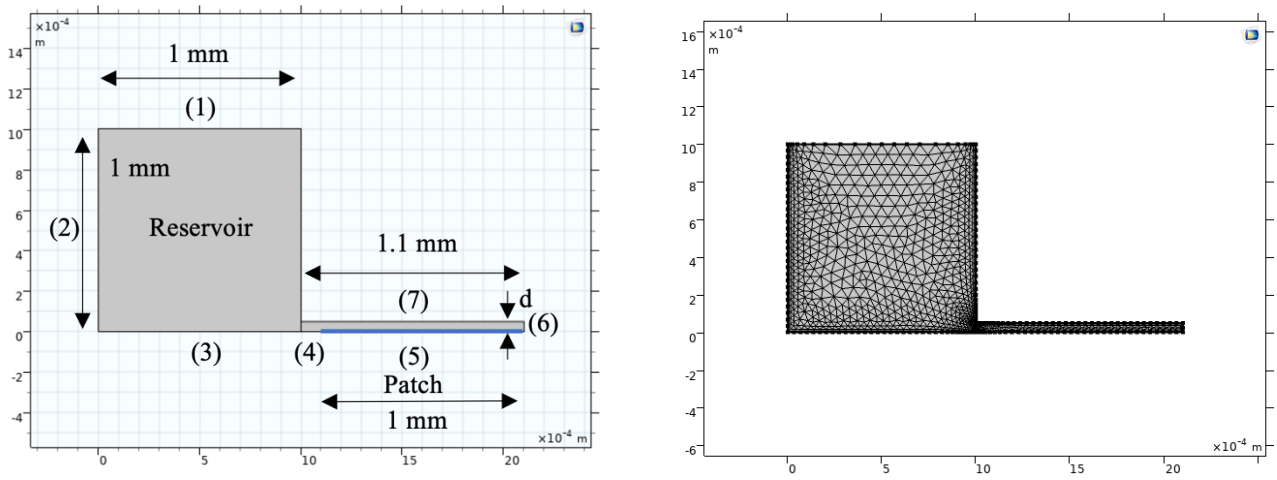

Figure 1. (Left) 2D geometry model of the biosensor system with relevant dimensions and boundaries. (Right) Mesh with variable mesh density used for the simulations.

smaller than its length and the dimensions of the reservoir. A higher mesh density along the y-direction can be used to aid in convergence.

Physical Models and Boundary Conditions. Flow in the reservoir and in the microchannel is modelled as time-dependent laminar flow. Both velocity driven flow (constant volumetric flow rate Q = 10 nL/s) and pressure driven flow (P = 1000 Pa) are simulated. A no-slip wall boundary condition is applied to boundaries (2),(3), (4), (5) and (7); inlet boundary condition (fixed pressure or fixed velocity) is applied at boundary (1) and an outlet boundary condition (p = 0) is applied at boundary (6). The velocity at the inlet is determined as Q/A, where A = 1 mm^2. The initial velocity field within the domain is assumed to be 0.

The diffusion of nucleotides within the domain is modeled using a time-dependent transport of diluted species model. A no-flux boundary condition is applied at boundaries (1), (2), (3), (4), & (7), and an outlet boundary condition is applied at boundary (6). The initial concentration within the reservoir at t = 0 is assumed to be 1nM, and that within the microchannel is assumed to be 0. A flux boundary condition is applied at the biosensor patch boundary (5). The inward flux due to unbinding of the complex AbA is:

$$\frac{dc}{dt} = k_{\text{off}}[AbA] - k_{\text{on}}[Ab0 - AbA]c$$

Here, c is the concertation of the target molecule sin the sample, k_{on} and k_{off} are the association and dissociation rate constants respectively, [AbA] is the concentration of bound complex AbA and Ab0 represents the initial site concentration of the DNA sequences in the patch at t = 0.

At the biosensor patch, a boundary PDE in terms of the site surface concentration [AbA] is applied. The source term in this PDE is:

$$\frac{d[AbA]}{dt} = -k_{\text{off}}[AbA] + k_{\text{on}}[Ab0 - AbA]c$$

Here, the initial site concertation of the DNA sequences on the patch Ab0 at t = 0 and is set to be 1000/μm^2. The material within the domain is water. The diffusivity D of the target molecules is set to 1e-9 m^2/s. Geometric and physical parameters used in the modeling are listed in Appendix A.

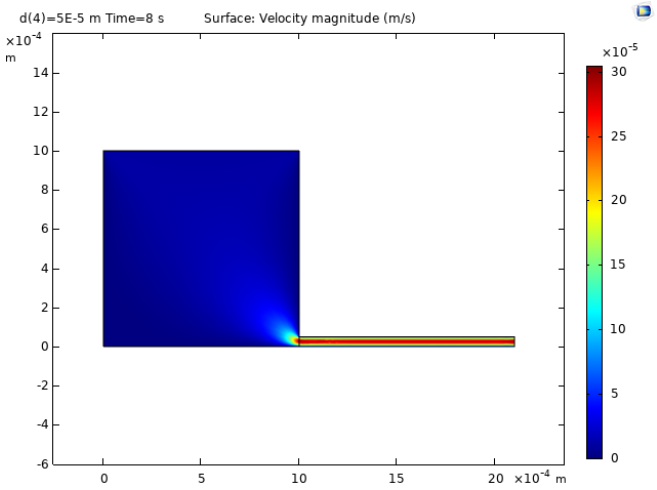

Figure 2. The variation of velocity in the reservoir and microchannel for velocity-driven flow at Q = 10 nL/s and microchannel height d = 50 μm.

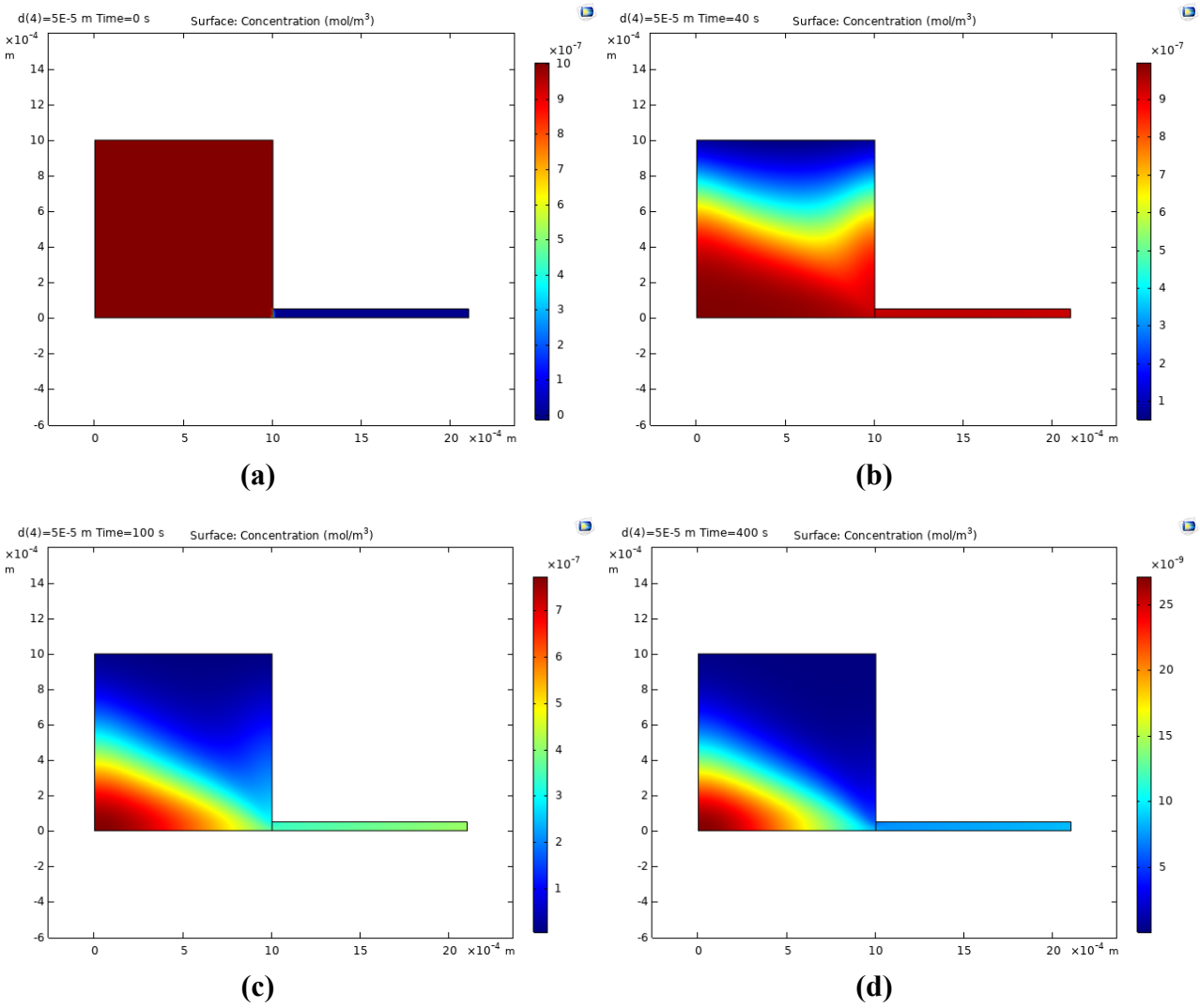

(a) **(b)** **(c)** **(d)**

Figure 3. The variation of solute concentration in the reservoir and microchannel for velocity-driven flow at Q = 10 nL/s and microchannel height d = 50 μm, at (a) t = 0, (b) t = 40s, (C) t = 100s and (d) t = 400s

Results and Discussion

Velocity-Driven Flow. Velocity-driven flow was simulated by setting a constant flow rate Q = 10 nL/s at the inlet of the reservoir. The simulations were carried at 4 different microchannel heights (d = {1, 5, 25, 50} μm). Increasing the microchannel height decreases the velocity of flow in the microchannel, given an increase in area for a constant flow rate. This decrease in microchannel velocity varies linearly with height of the microchannel d (since A = wd). In all cases, a parabolic velocity profile characteristic of laminar flow between parallel flat plates is observed within the microchannel, with zero velocity at the walls and a maximum velocity at the center of the microchannel (Figure 2). This flow profile is also observed for pressure-driven flow and can be characterized as Poiseuille flow. At the given flow rate, the convective effect of velocity is much stronger than the flux due to diffusion. This can be observed in figure 3, which variation of solute concentration in the reservoir and microchannel for velocity-driven flow at different times.

The total binding at the patch is determined from the line integral of the site concentration of the complex [AbA] at the patch. The variation of complex site concentration with time for 4 different microchannel heights given velocity-driven flow is shown in Figure 4. Increasing the height results in a lower value of the local maximum obtained, and the maximum is also achieved at a slightly later time. Therefore, in order to achieve the highest concentration of bound complex at the earliest time, a lower channel height is recommended. However, the deviation between the complex site concentration [AbA] at d = 1 μm and d = 50 μm is relatively small. Thus, the total amount of complex formed shows little deviation for changing microchannel height for velocity-

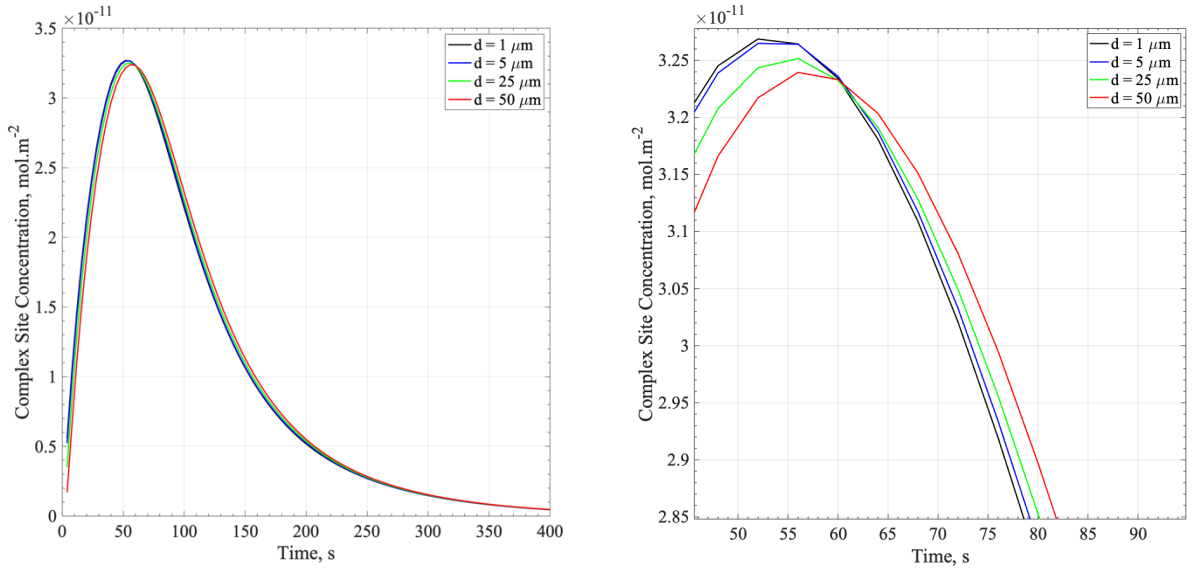

Figure 4. The variation of complex site concentration with time for 4 different microchannel heights given velocity-driven flow at volumetric floor rate = 1 nL/s.

driven flow. In each case, a local maximum is achieved at t ~ 55s. At this maximum, the net rate of production of complex AbA is zero, such that the rate of production of the complex matches the rate of consumption. This can be represented as:

$$k_{on}c(Ab0 - AbA_{max}) = k_{off}AbA_{max}$$

Pressure-Driven Flow. Pressure-driven flow was simulated by setting a constant pressure P = 1000 Pa at the inlet of the reservoir. A parametric study was performed for 5 different microchannel heights (d = {0.5, 0.75, 1, 2.5, 5} μm). The variation of complex site concentration with time for 5 different microchannel heights given pressure-driven flow is shown in Figure 5. Decreasing the microchannel height results in an increase in the maximum complex site concentration [AbA] achieved at the patch; the local maximum is also achieved at a later time for smaller microchannel heights. Thus, in order to increase the total amount of binding, a smaller microchannel height is recommended. In order to maximize the total binding at t ~ 30 mins (t = 1800 s) a channel height of d ~ 0.75 μm is recommended, since the local maxima is reached at t ~ 30 mins.

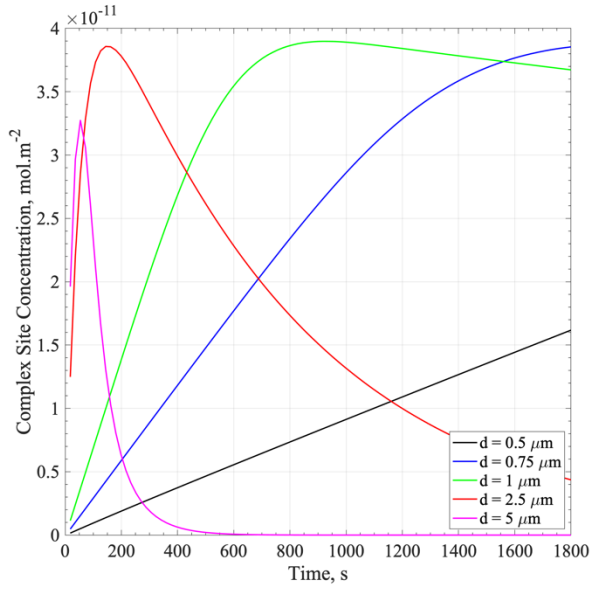

Figure 5. The variation of complex site concentration with time for 5 different microchannel heights given pressure-driven flow at P = 1000 Pa

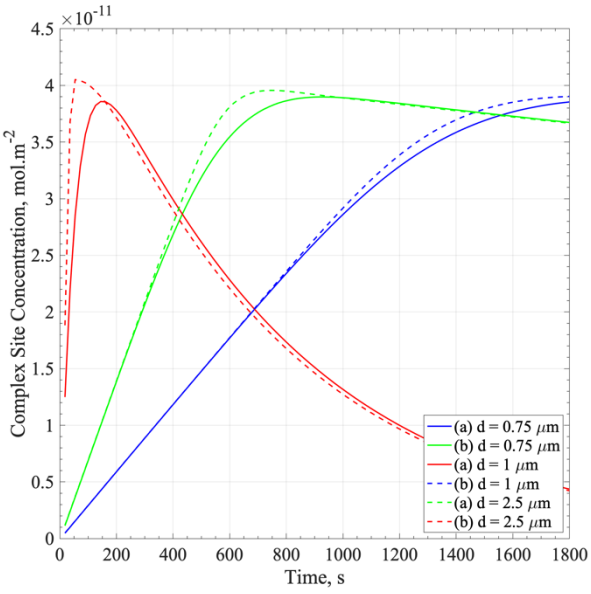

Figure 6. The variation of complex site concentration with time for $k_{on} = 100k_{on,1}$ and $k_{off} = 100k_{off,1}$, given pressure-driven flow

This behavior can be explained by looking at the combined Poiseuille-Couette flow relationship for pressure-driven flow between flat plates. For pressure-driven flow between parallel flat plates, the relationship between flow velocity, pressure and height of the channel can be written as:

$$v_x = \frac{\Delta P}{L}\left(\frac{yd - y^2}{2\mu}\right)$$

The maximum velocity occurs at y = d/2 and can be represented as:

$$v_{x,max} = \frac{\Delta P}{L}\left(\frac{d^2}{8\mu}\right)$$

Thus, for a given pressure drop across the microchannel the average velocity of flow within the channel varies as $v \sim d^2$. Thus, a small increase in the microchannel height *d* results in comparatively large changes in the velocity within the microchannel. The disparity between the characteristic diffusion time ($\sim d^2/D$) to the binding patch (y-direction) and the characteristic convection time ($\sim L/v$) in the x-direction becomes larger, causing the maximum binding to happen faster, and for the local maximum to be lower.

The total binding was then compared for higher dissociation and association rate constants ($k_{on} = 100k_{on,1}$; $k_{off} = 100k_{off,1}$). The variation of total bound complex site concentration with time for *d* = {0.75, 1, 2.5} μm is shown in Figure 6, and compared with the trend observed at lower k_{on} and k_{off} values. Here, the solid lines represent complex site concentration at $k_{on} = 10^6$ $M^{-1}s^{-1}$ and $k_{off} = 0.04$ s^{-1}, while the dotted lines represent complex site concentration at $k_{on} = 10^8$ $M^{-1}s^{-1}$ and $k_{off} = 4$ s^{-1}. The higher association/dissociation constants result in faster reaction, causing the local maximum in [AbA] value to be reached faster than at lower association/dissociation constant, but the value of the local maximum shows a small change (~5%). This behavior is expected because although the rates of the forward and backward reactions are increased, the value of $k_{on}/k_{off} = K_d$ remains constant.

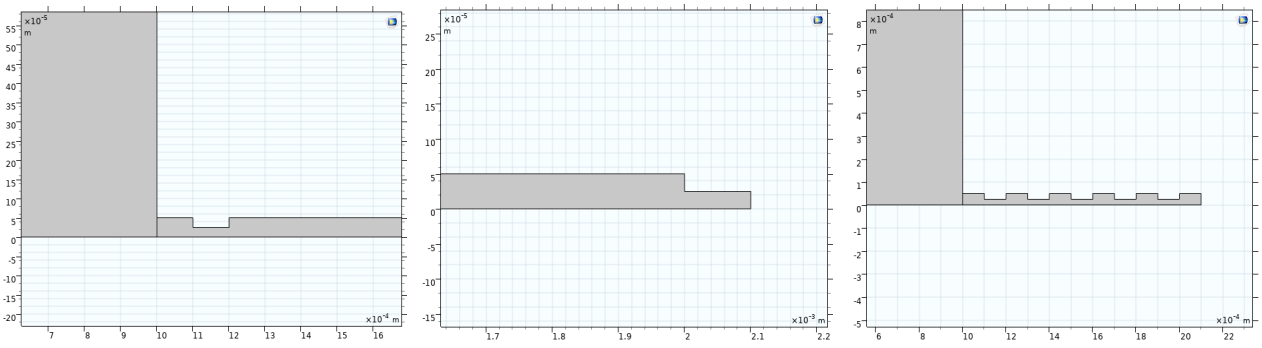

Figure 7. Different microchannel geometries (a) step added at patch entrance, (b) step added at patch exit; and (c) an array of 5 steps added along the patch.

Microchannel Geometry. The geometry of the microchannel was modified by adding steps to the top surface of the microchannel. Three scenarios were investigated – (a) step added at patch entrance, (b) step added at patch exit; and (c) an array of 5 steps added along the patch. The total height of the microchannel was kept constant at 1μm, and each step was assumed to have a height of 0.5 μm and width of 0.1 mm. The variation of the binding performance with time for the different designs is shown in Figure 8. Both the front and back step designs have the same effect on the total complex site concentration, resulting in a delay at which the local maximum is achieved. This behavior is expected because the velocity of flow is slowed by the same amount in both cases. The effect on the maximum binding achieved is small; this can be attributed to the fact that the dimensions of the step are small compared to that of the patch. However, introducing a single step, either at the front or the back results in a higher site concentration of complexes at collection time (t = 1800s), thus allowing us to remove more target molecules from the sample. Adding multiple steps, however, caused a significant fall in the site concentration at t = 1800s, compared to the case where there are no steps in the channel. Although this configuration performs better than a no-step configuration (d = 0.5 μm) at t < ~1000s, at the collection time of t =1800s, the complex site concentration is lower. Thus, this configuration is not recommended.

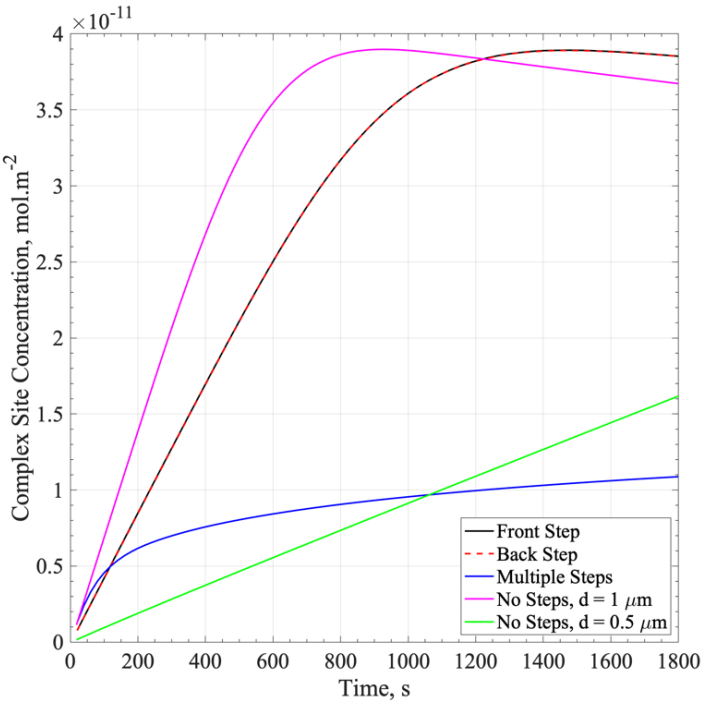

Figure 8. The variation of the binding performance with time for different microchannel designs

Similarly, a configuration where the steps have gradually changing depth can also be explored. However, the configuration is less likely to improve performance as well; since the effective diameter would be considerably lower, resulting in a lower total complex site concentration at the collection time. Since adding a single step allows us to maximize the total complex site concentration at t ~ 20-30 mins, adding multiple steps would only decrease the total complex site concentration at collection time.

Conclusions

In this report, the effect of microchannel height on the binding performance of a biosensor system was investigated. For velocity-driven flow at a constant flow rate, the effect of microchannel height was found to be small, although increasing the height was observe to result in a lower value of the maximum in complex site concentration obtained, and the maximum was also achieved at a slightly later time. For pressure driven flow at P = 1000 Pa, a smaller microchannel height was found to increase the maxim site concentration of the complex, and the maximum was observed at later time. The optimal value of microchannel height was found to $d \sim 0.75$ μm for collection at $t \sim 30$ mins. At this height, the complex site concentration is close to its maximum value at t = 1800s. Increasing the association/dissociation rate constants resulted in a small change in the maximum complex site concentration, but resulted in faster reaction, causing the maximum to appear earlier. Finally, the effect of microchannel geometry on binding performance was investigated. Adding a step either to the front or back of the microchannel was found to improve performance by delaying the location of the maximum, resulting in higher complex site concentration at the collection time of $t \sim 30$ min. Introducing multiple steps was found to cause a deterioration in performance, since the slower velocity resulted in a delay in the location of the maximum, causing complex site concentration at the collection time of $t \sim 30$ min to be comparatively lower.

Appendix A

Table 1. Geometric and physical parameters

d	variable	Microchannel Height
l	1.1 [mm]	Microchannel Length
H	1 [mm]	Reservoir Height
L	1 [mm]	Reservoir Length
A	1 [mm^2]	Reservoir Area (L * wdh)
c0	1 [nM]	Initial Solute Concentration
Ab0	1000 [1/um^2] / (6.023*10^23) [1/mol]	Initial Binding Site Density
kon	10^6 [M^-1/s]	Kon
koff	4*10^-2[1/s]	Koff
Q	10 * 10^-12 [m^3/s]	Volumetric Flow Rate
wdh	1 [mm]	Reservoir Width
l_gap	0.1[mm]	Step Length
h_gap	d/2	Step Height